Classification of Microstructures by Morphological Analysis and Estimation of the Hydration Degree of Cement Paste in Concrete

Alexandre Gonçalves Silva
Roberto de Alencar Lotufo
Franklin César Flores

FEEC–Faculdade de Engenharia Elétrica e de Computação
Universidade Estadual de Campinas
P.O.Box 6101, 13083-970
Campinas, SP - Brazil
{alexgs,lotufo,fcflores}@dca.fee.unicamp.br

Abstract. Cement is an essential material for the development of the civil construction. The analysis of cement-based materials is useful in the evaluation of mechanical properties, water absorption, air permeability and evolution of hydration degree. The latter is the motivation of this paper. New advantageous techniques of analysis based on the image information are possible using electronic microscopy. We propose here an alternative procedure to the segmentation of microstructures of cement and aggregates in concrete. The central idea consists of a particular use of the morphological operator watershed. We report the results of the analysis of about 450 Scanning Electron Microscope (SEM) images.

1 Introduction

The chemical composition of cement is controlled by the content of silica (SiO_2), lime (CaO), alumina (Al_2O_3) and iron (Fe_2O_3) oxides. Concrete basically is constituted of cement, aggregates and water. Hydration is reactions of cement with water resulting a firm and resistant matrix. Some approaches, for instance chemically bound water, X-ray diffraction and heat of hydration [15, 8], are availiable to characterise the hydration degree of cement-based materials. However, these methods can be only used at a given stage of hydration and, futhermore, require some assumptions concerning the chemical composition of the mixture [10]. The Scanning Electron Microscope (SEM) has been used to analyze the differences in microstructure, hydration degree [9, 10] and microcracks, of samples submitted to different types of curing. Image analysis, for this study, is a valuable option in relation to other techniques.

This paper consists of a classification of the concrete microestructures by semiautomatic methods. The aim is to detect two structures: aggregates grains and anhydrous grains. The hydrated phase is what ramins from these segmentations. Here a morphological approach is done based on the grayscale information. Special attention is given to the aggregate segmentation method. In the literature, the anhydrous segmentation is focused instead. The determination of anhydrous phase is important to estimate the hydration degree of cement while the aggegates segmentation is useful to analyze the type of composition of a strange (or not) concrete mixture. This has several implications for concrete characteristics.

Section 2 provides the theoretical foundation. In Section 3 our techniques are presented. Section 4 shows experimental results and some discussion about these results. Finally, the conclusions are drawn in Section 5. Here follows a preliminary overview illustrating the image acquisition method, visual structures observed and algorithms used.

1.1 Image Acquisition

The microscopic analysis was effected in polished sections of samples (cylinders of 10cm x 20cm) of hardened concrete in 28, 90 and 180 days. The samples are cut from the central portion. This slice is made by a diamond saw and has a diameter of 5cm and a height of 1cm approximately.

After that a sample is scanned in the SEM, the spread image is visualized in a monitor. The results are images of 640x480 pixels with 256 graylevels (8 bits) and a magnification of 100 times [9].

1.2 Visual Structures

Figure 1 illustrates an example of concrete image under SEM. Concrete is essentially composed by three parts: the anhydrous, which are composites of cement not hydrated (white pores); the aggregates that are not cement-components such as sand, stone or slag

(medium-gray homogeneous pores); and the hydrated composites that are the remaining portion. Aggregate structures have a maximal size previously defined (by a filtering process).

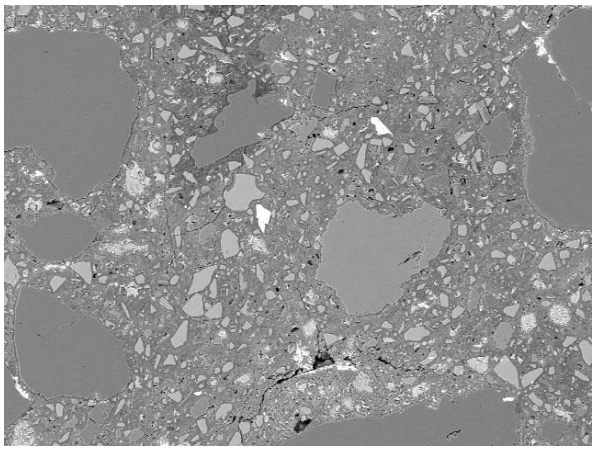

Figure 1: Example of concrete image under SEM.

1.3 Algorithms Overview

The algorithms are briefly presented in this subsection.

Anhydrous grain segmentation is implemented by image histogram processing, thresholding by the watershed technique, followed by area opening.

To process the aggregate segmentation, connected basins of image gradient are removed, watershed with regional minimum as marking is applied and, area opening and area closing are determined.

2 Preliminary Definitions

Let $E \subset \mathbf{Z} \times \mathbf{Z}$ be a rectangular finite subset of points. Let $K = [0, k]$ be a totally ordered set. Denote by $Fun[E, K]$ the set of all functions $f : E \to K$. An *image* is one of these functions (called graylevel functions). Particularly, if $K = [0, 1]$, f is a binary image. An *image operator* (*operator*, for simplicity) is a mapping $\psi : Fun[E, K] \to Fun[E, K]$.

Dilation and *erosion* are morphological operators [6, 4] and are denoted, respectively, by δ_B and ε_B throughout this text.

A grayscale operator ψ is considered an *morphological filter*, if ψ is increasing and idempotent, or, if $f_1 \leq f_2 \Rightarrow \psi(f_1) \leq \psi(f_2)$ and $\psi\psi(f) = \psi(f)$.

The *opening* and *closing* operators [6, 4] are morphological filters and are denoted, respectively, by γ_B and ϕ_B.

Let $N(x)$ be the set containing the *neighbourhood* [7, 4] of x, $x \in E$. We define a *path* [7] from x to y, $x, y \in E$ as a sequence $C = (p_0, p_1, ..., p_n)$ from E, where $p_0 = x$, $p_n = y$ and $\forall i \in [0, n-1], p_i \in N(p_{i+1})$.

A *connected subset* of E is a subset $X \subset E$ such that, $\forall x, y \in X$, there is a path C entirely inside X.

Let $f \in Fun[E, K]$. A *flat zone* of f is a connected subset $X \subset E$, such that $f(x) = f(y)$, $\forall x, y \in X$.

Definition 1 *Let $f \in Fun[E, K]$. ψ is said to be a connected operator if and only if*

$$f(x) = f(y) \Rightarrow \psi(f)(x) = \psi(f)(y)\,,$$

where $x, y \in E$, $x \in N(y)$.

Connected filters reduce the number of flat zones [2, 13, 6, 11] without introducing borders. Notice that when some flat zones in an image are reduced, some borders may be supressed, but it does not seem to create new borders.

Definition 2 *The sup-reconstruction operator is given by, $\forall f, g \in Fun[E, K]$,*

$$\phi_{B_c,f}(g) = \varepsilon^{\infty}_{Bc,g}(f)\,,$$

where $B_c \subset E$ is the structuring element defining connectivity, $n \in \mathbf{Z}_+$ and $\varepsilon^n_{B_c,g}$ is the n-conditional erosion operator [14, 5]. $\varepsilon^{\infty}_{B_c,g}(f)$ means that the erosion is applied till idempotency.

Definition 3 *Let $f \in Fun[E, K]$. A regional minimum is a flat zone Z such that $f(z) < f(n)$, $z \in Z$, $n \in N, N \in \mathcal{F}_Z$, where $\mathcal{F}_Z$ is a set of all flat zones adjacent to Z [4]. The regional maxima of f is found by application of a operator $\mu^{\min}_{B_c} : Fun[E, K] \to Fun[E, [0, 1]]$, given by*

$$\mu^{\min}_{B_c}(f) = (1 \leq (\phi_{B_c,f}(f-1) - (f-1))) \vee (f \leq 0)\,,$$

where $\phi_{B_c,f}$ is a sup-reconstruction.

Definition 4 *Let $f \in Fun[E, K]$, $x \in E$, $k \in \mathbf{R}$, the threshold decomposition is defined by*

$$\tau_k(f) = \begin{cases} 1\,, & if\ k \leq f(x) \\ 0\,, & otherwise \end{cases}\,.$$

Definition 5 *Let $f \in Fun[E, K]$, $K = [0, k]$, and $x \in E$, the negative operator is defined by*

$$\nu(f) = k - f(x)\,.$$

Notice that, when $k = 1$ (binary images), $\nu(f)$ is the set-complement of f.

Definition 6 *Let $x \in E$, $\partial E_{d_h,d_w} \subset E$, the frame image is created as to following:*

$$fr(x) = \begin{cases} 1\,, & if\ x \in \partial E_{d_h,d_w} \\ 0\,, & otherwise \end{cases} ,$$

where d_h is the width thickness in left and right borders, and d_w is the height thickness in top and bottom borders.

Definition 7 *Let $f \in Fun[E,K]$. Let us consider the histogram of the image as a function $h_f : K \to \mathbf{Z}_+$ given by*

$$h_f(i) = card\{x \mid f(x) = i\}$$

where $card(x)$ is the cardinality of x. Despite the domain of h_f, the morphological operators used in the graylevel classification were applied in the same manner. In other words, we consider K as a subset of E.

2.1 Morphological Operators

In this subsection we introduce the morphological operators used in this work.

2.1.1 Alternating Sequencial Filtering

The *alternating sequential filtering*, $\forall f \in Fun[E,K]$, and for every structuring element B, is given by

$$\mu_{k,B}(f) = \pi_k \pi_{k-1} \cdots \pi_1(f) \quad and$$

$$\upsilon_{k,B}(f) = \rho_k \rho_{k-1} \cdots \rho_1(f)\,,$$

where

$$\pi_k(f) = \gamma_{kB}\left(\phi_{kB}\left(\gamma_{kB}\left(f\right)\right)\right)\,,$$

$$\rho_k(f) = \phi_{kB}\left(\gamma_{kB}\left(\phi_{kB}\left(f\right)\right)\right) \quad and$$

$$kB = \begin{cases} (origin), & for\ k = 0 \\ \underbrace{\delta_B\left(\delta_B\left(\cdots \delta_B\left(B\right)\right)\right)}_{k-1\ dilations}, & for\ k \geq 1 \end{cases} .$$

This filtering is frequently used to smooth the topographic surface of an image. In other words, this may be desirable in order to reduce noise or simplify grayscale variation in a preprocessing stage.

2.1.2 Area Opening / Area Closing

The *area opening* is a connected filter applied to binary images, aiming to eliminate flat zones valued 1 and with area lower than a threshold a. Let $\mathcal{B}$ be the set of all flat zones valued 1 in a binary image. Let $a \in \mathbf{Z}_+$ be an area threshold. Let $\mathcal{B}_a \subset \mathcal{B}$ be the set of all flat zones $F \in \mathcal{B}$ whose area is greater than a. Let $f \in Fun[E,K]$, the area opening operator is given by

$$\gamma_a^{\text{area}}(f) = \bigvee_{F \in \mathcal{B}_a} \gamma_F(f)\,.$$

The dual operator of area opening is the *area closing*. This filter is a mapping Φ_a^{area}, given by

$$\phi_a^{\text{area}}(f) = \nu(\gamma_a^{\text{area}}(\nu(f)))\,.$$

2.1.3 h-Basin

This operator sup-reconstructs the grayscale image f from the marker created by the addition of the positive integer value h to f, using the connectivity B_c. It removes connected basins with a contrast smaller than h. This function is very useful for simplifying the basins of the image.

$\forall f \in Fun[E,K]$, *h-basin* is determined by

$$h\_\phi_{B_c,h}(f) = \phi_{B_c,f+h}(f)\ .$$

2.1.4 Morphological Gradient

The *morphological gradient*, $\forall f \in Fun[E,K]$, and for every structuring element B_{dil} (of dilation) and B_{ero} (of erosion), is given by

$$\Psi_{B_{dil},B_{ero}}(f) = \delta_{B_{dil}}(f) - \varepsilon_{B_{ero}}(f)\,.$$

This operator is frequently used to enhance contours or non homogeneous regions.

2.1.5 Watershed

The *watershed* [1, 16] is a powerful tool of segmentation. It is based on the concept that any grayscale image can be considered as a topographic surface. If we flood this surface from its markers and, if we prevent the merging of the waters coming from different sources, we partition the image into two different sets: the catchment basins and the watershed lines.

We will use the symbol $W_m(f)$ to represent the watershed operator. m is the image of markers and the *3x3 cross* structuring element (B_{cr}) is used.

3 The Proposed Technique

In this section, we describe each step of our proposed techniques. Subsection 3.1 and Subsection 3.2 present, respectively, our anhydrous and aggregates segmentation method.

3.1 Anhydrous Segmentation

There are many techniques for global thresholding determination. In particular, we can cite the entropy maximisation and ISODATA used by Mouret [10, 9]. Here, we use a morphological approach to detection of domes in a histogram.

We can observe that the histogram in Figure 2a (calculated from image of Figure 1) has a small peak in

the white region related to the anhydrous phase. This information is similar in almost all images under a controlled process of acquisition resolution of a determined concrete mixture composition.

The threshold value is extracted using the watershed technique. The aim is to detect the middle valley of the histogram. If the histogram is negated, we need to extract the middle peak of the one dimensional signal. This is accomplished by finding proper markers on the valleys. These markers are extracted by detecting the regional minima of the filtered signal (alternating sequential filtering, closing followed by opening):

$$h_{asf} = \upsilon_{1,B_{line8}} \left(\nu \left(h_f \right) \right) \ ,$$

where B_{line8} is a line of length 8 pixels. It represents 1/32 (or 3%) of 256 (greatest graylevel discriminated by h_f). This value is sufficient to create regional minima conveniently in various histograms. Figure 2b shows this filtering result. After, the watershed is applied in h_{asf}.

$$ws = W_m \left(h_{asf} \right) \ ,$$

where m is the default markers of classic watershed defined by regional minima:

$$m = \mu_{B_c}^{min} \left(h_{asf} \right) \quad and \quad B_c = B_{cr} \ .$$

Figure 2c shows the watershed result. To discard the detection of peaks near the limits of the histogram, an intersection is done using an border image negated with appropriated width:

$$wsf = \min \left(\{ fr \mid \partial E_{0,20} \subset E \}, ws \right)$$

The coordinate value is detected by

$$k_{th} = \{ x \mid wsf(x) = 1 \}$$

For illustrative purpose, a plot of h_f and wsf signals are displayed in Figure 2d.

The threshold value found in the previous step is applied. Figure 3a shows a example of image and Figure 3b shows thresholding result ($\tau_{k_{th}} (f)$). After, a filter is applied to remove sufficiently small blobs (area less than 20).

$$anhy = \gamma_{20}^{area} \left(\tau_{k_{th}} \left(f \right) \right)$$

For illustration, the anhydrous grains are displayed (in white) in Figure 3c.

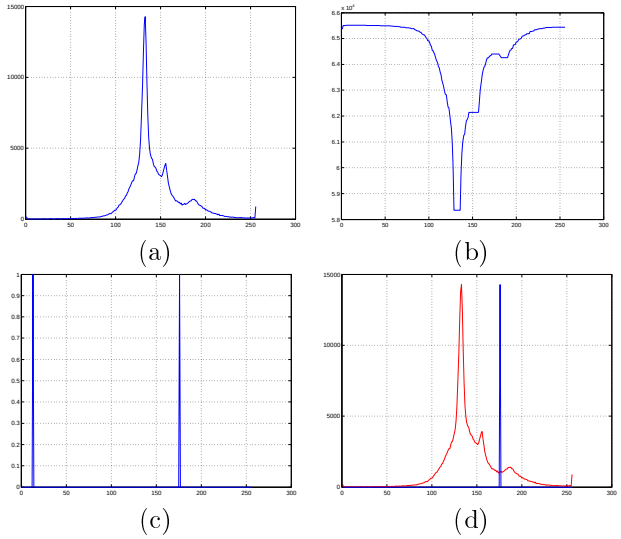

Figure 2: (a) Histogram of image of Figure 1 (b) Filtering of negated histogram (c) Watershed lines on filtered signal (d) Threshold value found, put on the histogram

3.2 Aggregates Segmentation

Now, the objective is to detect the aggregate phase which is the main responsible for the unitary mass, elasticity module and dimensional stability of concrete [12]. There is a certain difficulty here because a global thresholding is not possible in this case. The difference between aggregate and hydrated paste is that the first is homogeneous and the second has texture. The technique proposed here is the greatest contribution of this paper.

The watershed applied on the gradient using the markers from filtered regional minima of the gradient is a standard watershed based technique. In this case the filter was chosen to be a contrast h-basin:

$$grad = \Psi_{B_{cr},B_{cr}} \left(f \right)$$

$$m_a = \mu_{B_{cr}}^{min} \left(h\_\phi_{B_{cr},h_m} \left(grad \right) \right)$$

$$ws_a = W_{ma} \left(grad \right)$$

where h_m is determined manually depending on the concrete type (h_m is around of 20).

Figure 4a shows these watershed lines (in white) and the surfaces of markers (in gray).

The result of the watershed in the previous step is the detection of a large number of regions. Figure 4b shows the larger ones that are the aggregates and the anhydrous. So first the regions are filtered out using an area criteria, and small holes are closed:

$$a_1 = \gamma_{300}^{area}\left(\nu\left(ws_a\right)\right)$$

$$a_2 = \phi_{50}^{area}\left(a_1\right)$$

The aggregates are obtained by removing the anhydrous phase:

$$aggr = a_2 - anhy$$

For illustration, the aggregates are displayed (in white) in Figure 4c.

Finally we have each phase of concrete structures. The third phase is hydrated composites and can be denoted by

$$hydcomp = f - a_2\ .$$

4 Experimental Results

In this section we present estimated values of the percentage of anhydrous grains, aggregates and hydration degree. The images are obtained from two types of cement and three types of curing in a concrete mixture. For this study, 450 images were analyzed. Table 1 shows some these results. The used notation is explained here:

The area is calculated by

$$A_{f_{bin}(x)} = \sum_{\forall x \in E} f_{bin}\left(x\right)\ ,$$

and the normalized area (or area fraction) is

$$a_{f_{bin}} = \frac{A_{f_{bin}}}{card\left(E\right)}\ ,$$

where $f_{bin} \in Fun\left[E,[0,1]\right]$, and $card(E)$ is the cardinality of E. Therefore, a_{anhy} and a_{aggr} are the anhydrous and aggregate phases of area fraction.

The estimated hydration (α) degree based on image treatment is written by [9, 3]

$$\alpha = 1 - \frac{a_{anhy}}{\Gamma_0}\ , \quad \Gamma_0 = \frac{C}{C + \rho_c \cdot a}\ ,$$

where C is the cement consumption per m^3 of concrete, a is the water consumption per m^3 of concrete, and ρ_c is the specific mass of cement.

Important: this is true at 400 times magnification. In our case (100 times), this normalization of anydrous grains (a_{anhy}) is increased by 17% [9].

Type	Cure	Age	a_{anhy}	a_{aggr}	$\overline{\alpha}$
t_1	c_1	28	0.109	0.411	0.561
t_1	c_1	90	0.113	0.159	0.670
t_1	c_1	180	0.076	0.368	0.673
t_1	c_2	28	0.089	0.220	0.663
t_1	c_2	90	0.078	0.273	0.727
t_1	c_2	180	0.054	0.366	0.740
t_2	c_1	28	0.091	0.225	0.759
t_2	c_1	90	0.041	0.486	0.812
t_2	c_1	180	0.037	0.300	0.863
t_2	c_2	28	0.077	0.182	0.737
t_2	c_2	90	0.058	0.205	0.818
t_2	c_2	180	0.036	0.193	0.862

Table 1: t_1 is Portland blast furnace cement; t_2 is Portland high initial resistence cement; c_1 is humid curing during 7 days; c_2 is steam thermal curing (60^o); $\overline{\alpha}$ is the medium hydration for each type of concrete (above 10 images considering the first three columns)

4.1 Discussion

A similar image analysis process is reported by Mouret [10]. His work concentrates on the anhydrous phase segmentation that is the goal for hydrated degree estimation. His algorithm is based on the thresholding by entropy maximisation of greylevel (maximisation of the histogram contrasts) of the image intensity filtered, followed by hole closing (of the anhydrous phase which may be hidden). Our technique also works with histogram, but a morphological analysis is made of the histogram. Mouret also mentions another work which uses the ISODATA technique to estimate the threshold to separate the anhydrous phase. Our techinque is very convenient if there is a dome in the histogram representing the anydrous phase. We found that for some concrete samples, the histogram did not reveal any dome and our method could not be applied.

On the other hand, our proposed technique to segment the aggregates based on the watershed transform gave excellent results, despite the manual choice of h_m. Aggregate particle shape, size, and gradation can impact the performance of concrete. In concrete mixtures, the characteristics of aggregate phase has been related to permanent deformation, and fatigue resistance. The properties that are affected include stiffness, stability, durability, permeability, resistance to moisture damage, and air voids in the mix. To design concrete mixtures with long service lives, the aggregates must have the proper gradation and shape. This study also can be used in analysis of the aggregate influence.

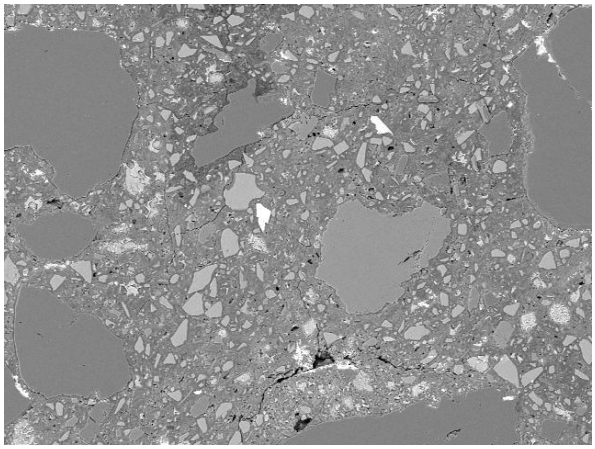

(a)

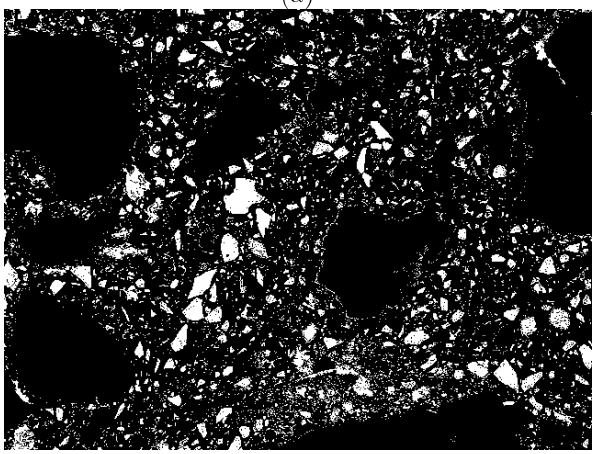

(b)

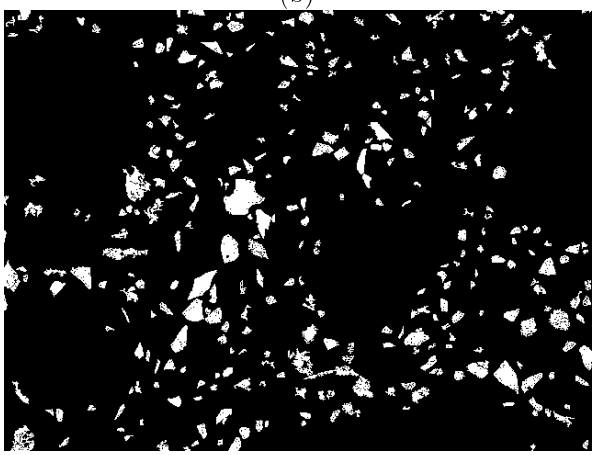

(c)

Figure 3: (a) Original image (b) Thresholding result (c) Anhydrous segmentation

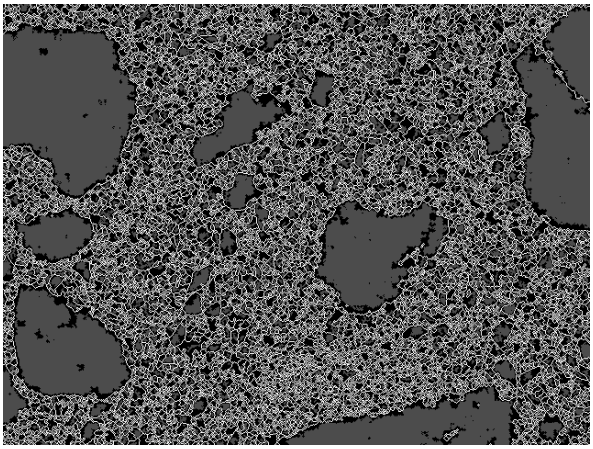

(a)

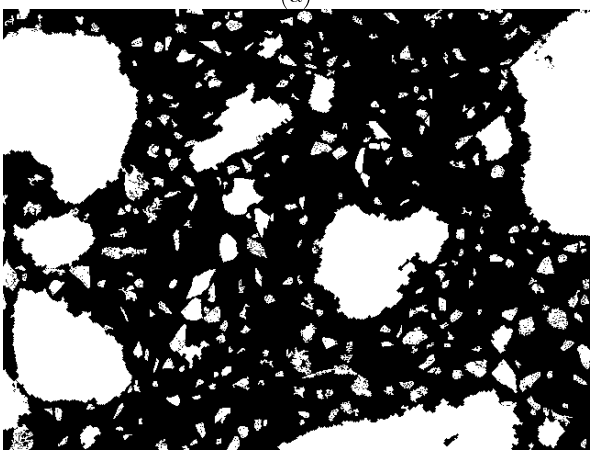

(b)

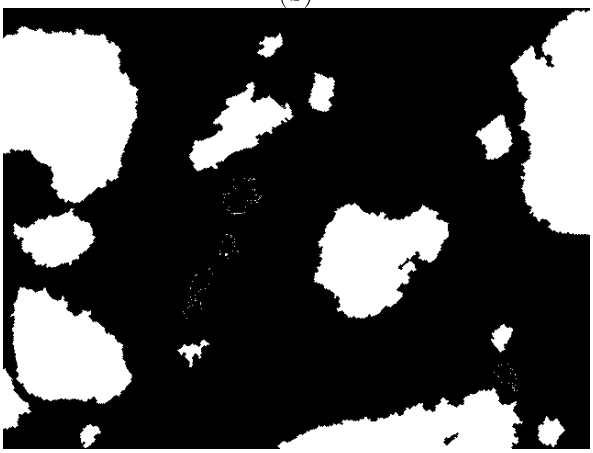

(c)

Figure 4: (a) Watershed lines and markers in gray (b) Agglomerated of Anhydrous and Aggregates (c) Aggregates segmentation

Figure 5 illustrates other example images from the segmentation presented in this paper. The pixels of segmented images are shown with the original image values.

5 Conclusions

We have presented an image analysis methodology for the classification of microstructures of cement paste from SEM image. The image segmentation first estimates the anhydrous composites, based on a global thresholding. The threshold is selected from a morphological histogram processing. The second segmentation is to detect the aggregate material, which has almost the same gray scale distribution as the hydrated material. We have proposed a watershed based segmentation which discriminates the texture of both materials.

These techniques were applied to estimate the anhydrous phase of several types of Portland cement with cure process and at different curing age. The image segmentation methodology proved very suitable for this task which was confimed by the analysis of approximately 450 SEM images.

Further work is required to improve the global threshold method to segment the anhydrous phase and to design an automatic procedure to estimate the parameter h_m used in the aggregate segmentation.

6 Acknowledgments

This work was an important tool (in particular, the topic about hydration degree) to the results of the Fernando Freitas' master thesis [3]. The images in this paper were kindly provided by Professor Gladis Camarini. We thank both researchers from the University of Campinas (FEC-Unicamp). We also thank Rachel for revision of this text. Alexandre G. Silva is supported by FAPESP under process 00/13671-0. Franklin C. Flores is supprted by CNPq under process 141899/2001-8.

References

[1] S. Beucher and F. Meyer. *Mathematical Morphology in Image Processing*, chapter 12. The Morphological Approach to Segmentation: The Watershed Transformation, pages 433–481. Marcel Dekker, 1992.

[2] J. Crespo, R. W. Schafer, J. Serra, C. Gratind, and F. Meyer. The flat zone approach: A general low-level region merging segmentation method. *Signal Processing*, 62(1):37–60, October 1997.

[3] F. A. E. de Freitas. Hidratação e Microfissuração, com o Auxílio da Análise de Imagens, em Concre-

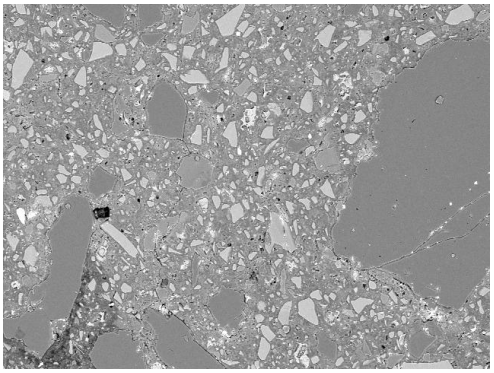

(a)

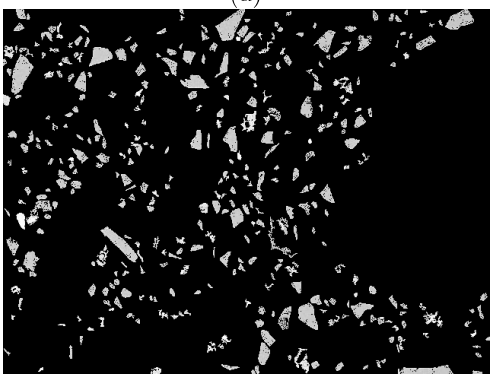

(b)

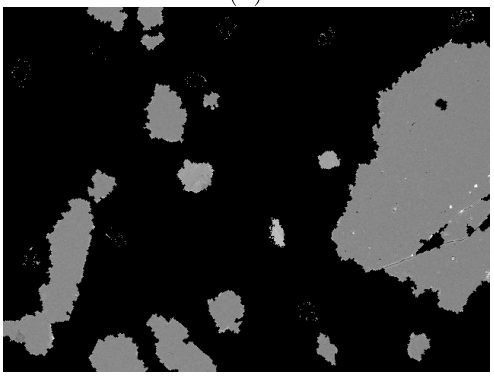

(c)

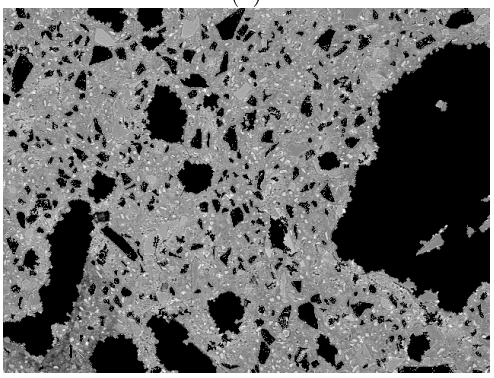

(d)

Figure 5: (a) Original image (b) Anhydrous segmentation (c) Aggregates segmentation (d) Hydrated phase

tos de Cimento com e sem Adição de Escória de Curados Termicamente. Dissertação de Mestrado, Faculdade de Engenharia Civil - Universidade Estadual de Campinas, August 2001.

[4] F. C. Flores. Segmentação de Seqüências de Imagens por Morfologia Matemática. Dissertação de Mestrado, Instituto de Matemática e Estatística - Universidade de São Paulo, Outubro 2000.

[5] H. J. A. M. Heijmans. *Morphological Image Operators*. Academic Press, Boston, 1994.

[6] H. J. A. M. Heijmans. Introduction to Connected Operators. In E. R. Dougherty and J. T. Astola, editors, *Nonlinear Filters for Image Processing*, pages 207–235. SPIE–The International Society for Optical Engineering, 1999.

[7] R. Hirata Jr. Segmentação de Imagens por Morfologia Matemática. Dissertação de Mestrado, Instituto de Matemática e Estatística - USP, março 1997.

[8] L. E. Copeland, D. L. Kantro, G. Verbeck. Chemistry of Hydration of Portland Cement. In *Proceedings of the Fourth International Symposium on the Chemistry of Cement*, volume 1, pages 429–65, 1960.

[9] M. Mouret, A. Bascoul and G. Escadellas. Study of the Degree of Hydration of Concrete by Means of Image Analysis and Chemically Bound Water. *Advanced Cement Based Materials*, 27(12):1851–1859, November 1997.

[10] M. Mouret and A. Bascoul. Image Analysis: a Tool for the Characterisation of Hydration of Cement in Concrete - Metrological Aspects of Magnification on Measurement. *CECO - Cement & Concrete Composities*, pages 1–6, October 2000.

[11] F. Meyer. From Connected Operators to Levelings. In H.J.A.M. Heijmans and J.B.T.M. Roerdink, editors, *Mathematical Morphology and its Applications to Image and Signal Processing*, Proc. ISMM'98, pages 191–198. Kluwer Academic Publishers, 1998.

[12] P. K. Mehta and P. J. M. Monteiro. Concreto: Estrutura, Propriedades e Materiais. *PINI*, page 573, 1994.

[13] P. Salembier and J. Serra. Flat Zones Filtering, Connected Operators, and Filters by Reconstruction. *IEEE Transactions on Image Processing*, 4(8):1153–1160, August 1995.

[14] J. Serra. *Image Analysis and Mathematical Morphology*. Academic Press, 1982.

[15] T. C. Powers and T. L. Brownyard. Studies of the Physical Properties of Hardened Portland Cement Pastes. In *ACI J. Proc.*, pages 1–9, 1948.

[16] L. Vincent and P. Soille. Watersheds in Digital Spaces: An Efficient Algorithm Based on Immersion Simulations. *IEEE Transactions on Pattern Analysis and Machine Intelligence*, 13(6):583–598, June 1991.